

# A Comparative Study on Heat Transfer and Friction Factor Characteristics of Silicon Carbide-water Nanofluids in a Circular Tube Fitted

Sneha Ponnada<sup>a,\*</sup>, Subrahmanyam Tunuguntla<sup>b</sup>, Sureddy Vishveshwara Naidu<sup>b</sup>

<sup>a</sup> Centre for Nanotechnology, AUCE (A), Andhra University, Visakhapatnam-530003, India

<sup>b</sup> Department of Mechanical Engineering, AUCE (A), Andhra University, Visakhapatnam-530003, India  
 p.sneha@ymail.com

The effect of perforated twisted tapes with alternate axis (PATT), perforated twisted tapes (PTT) and regular twisted tapes (TT) with twist ratios (TR) of 3 are compared by an experimental investigation in a circular tube with Silicon carbide (SiC)-water nanofluid flowing in it under constant heat flux condition. Using 0.1 wt. % concentration of the SiC nanofluid containing SiC nanoparticles obtained after 5 h of ball milling as the testing fluid, experiments are conducted within the Reynolds number range of 3000 – 16000. The heat transfer rates in the tube fitted with TT, PTT and PATT at TR = 3 are respectively improved up to 9.59 %, 18 % and 19.51 % of that in the plain tube. Similarly, the increase in friction factor for TT, PTT and PATT at a TR = 3 is 22.5 %, 24 % and 28.9 % respectively, compared to that of the plain tube. As PATT is giving maximum heat transfer enhancement, the empirical correlations were established for its Nusselt number and friction factor at different twist ratios and the obtained correlations are fitted with the experimental data. Hence, the passive elements when employed along with the nanofluid gives better energy efficiency along with lower operating cost and is therefore suggested for commercial heat transfer applications.

## 1. Introduction

The heat transfer enhancement of the fluids has been developed and applied for many heat exchange systems. There are many ways in which the heat transfer can be enhanced and among them, the use of nanofluids and the use of passive elements in the heat pipes and heat exchangers are of prime importance as they have reported a reasonable improvement in the heat transfer coefficient.

Nanofluids are the fluids containing nanoparticles of higher thermal conductivity and they reported a greater enhancement in the thermal properties when compared to the conventional heat transfer fluids like water, ethylene glycol and a combination of both. The heat transfer rates obtained by the different combinations of nanoparticles and the base fluids are being studied by many researchers. Hence, the conventional fluids for cooling and heating purposes are replaced by many newer fluids. Among the various nanoparticles, Silicon Carbide (SiC) is one of the promising materials employed to fabricate effective nanofluids as SiC is easily available and has a higher thermal conductivity. Not much research is done on the SiC/water for analysing the heat transfer coefficient of the nanofluid. (Yu et al., 2009) have reported results for 3.7% concentration of 170 nm SiC particles suspended in water at constant Reynolds number. (Timofeeva et al., 2010) have stated that the use of a SiC/water nanofluid will be beneficial in the laminar flow regime when particles are larger than ~50 nm, while for turbulent flow average particle sizes should be larger than ~90 nm. In their later work, (Timofeeva et al., 2011) have also reported investigations on SiC/water nanofluid over the base fluid with 90 nm SiC particle at 4 vol.%. (Muhammet et al., 2014) have stated results for the enhancement in the heat transfer coefficient at constant Reynolds number for SiC at 9 wt. % in water-ethylene glycol base fluid.

The researchers have investigated on many passive elements i.e., inserts and have reported their investigations. Among them, different types of twisted tapes are employed and studied as they are easy manufacture due to their non-complex configuration and will result in a relatively lower pressure drop. For the heat transfer improvement some modifications are done on the conventional tapes. A report on Nusselt

number and friction factor increase with decreasing twist ratios, width ratios and increasing depth ratios for V-cut twisted tapes was done by (Murugesan et al., 2011; Eiamsa-ard et al., 2010) have reported that multiple TT vortex generators lead to increase in heat transfer rate over the use of smooth channel from 10.3 to 169.5% and the friction factors are in the range of 1.45 and 5.7 times of those for the smooth channel. (Eiamsa-ard et al., 2010) have seen that the average Nusselt number and friction factor increase in the tube fitted with the full-length dual TT elements in tandem at  $y/w = 3.0, 4.0$  and  $5.0$ , are respectively 146%, 135% and 128%; and 2.56, 2.17 and 1.95 times than in the plain tube. And also, the short length twisted tape inserts as reported by (Eiamsa-ard et al., 2009) have a lower heat transfer rate and friction factor when compared to the full-length tapes, twisted tapes consisting of centre wings and alternate axis. (Eiamsa-ard et al., 2010) also stated that among the peripherally-cut TT, the Nusselt number of peripherally cut TT with alternate axis, peripherally cut TT and TT is enhanced up to 184%, 102% and 57% of that of the plain tube and the friction factor of peripherally cut TT with alternate axis increased 6 to 11 times that of the plain tube. (Eiamsa-ard et al., 2011) have examined alternate clockwise and counter-clockwise TT and observed that they yield higher Nusselt numbers than TT by around 70.9 to 104.0% and the Nu and friction factors are found to be higher than that of TT for the same twist ratio.

The use of twisted tape with alternate axis in combination with a trapezoidal wing are reported to give a heat transfer and friction factor increase of 2.84 and 8.02 times respectively to that of the plain tube, when experiments are conducted by (Khwanchit et al., 2011; Eiamsa-ard et al., 2018) worked on rectangular-cut twisted tapes with alternate axes (ARC-TTs) and reported that ARC-TTs yield higher Nu than TT by around 14.68% to 38.85% but lower than 2.16-10.88% than the alternate axis twisted tape. (Kumar et al., 2017) have experimented on square wings in multiple square perforated twisted tapes and reported 6.96 times increase in the Nusselt number and 8.3 times increase in the friction factor for the multiple square perforated TT inserts with square wings with a perforated width ratio of 0.25 and a twist ratio of 2.5. Similarly, (Amar Raj Singh Suri et al., 2018) have experimented on square wings in multiple square perforated twisted tapes and reported 5.92 times increase in the Nusselt number and 7.89 times increase in the friction factor for the multiple square perforated TT inserts with square wings with a perforated width ratio of 0.0833 to 0.333 and a twist ratio range of 2.0 to 3.5.

There is a modification of the conventional twisted tape inserts, which are employed in a heat pipe operating in the flow regime with Reynolds number range of 3000-16000 in the current work. The thermal performance of water in a circular tube with twisted tapes, perforated twisted tapes and perforated twisted tapes with alternate axis is reported by (S Ponnada et al., 2019). And the enhancement of heat transfer and friction factor of SiC nanofluid at 0.1 wt. % concentration containing particles ball milled after 5 h is circulated in a plain tube containing twisted tapes, perforated twisted tapes and perforated twisted tapes with alternate axis are then compared.

## 2. Characterization and thermo-physical properties of the nanofluid

A detailed study on the thermal phenomena of the nanofluids along with the characterization of SiC nanoparticles before and after dispersing in distilled water (DIW) is done. The pH of the fluids is adjusted to be between 9-10 before and after sonication. The sonication of the nanofluid is done by using a probe sonicator.

The stability of the suspensions is measured and analysed. The crystallite size of SiC particles obtained after 5 h, 10 h and 15 h ball milling are 27 nm, 39 nm and 62 nm respectively from XRD analysis. The particles are mostly indexed for a hexagonal crystal structure. The nanofluids are prepared at different concentrations of 0.04 wt. %, 0.08 wt. % and 0.1 wt. % as they have reported a better stability from the zeta potential analysis and a relatively lesser particle size from dynamic light scattering (DLS) results. The stability of the nanofluids is measured from a zetasizer Nano ZS90. The visual inspection technique is employed to study the sedimentation behavior of the nanofluids. The SiC nanofluids are then tested for thermal conductivity (TC) in a KD2Pro thermal conductivity analyzer and viscosity in a Physica MCR 51 rheometer.

The maximum increase in thermal conductivity (TC) and viscosity of the nanofluids with that of the base fluid at 0.1 wt. % is 19 % and 94 % respectively at 30 °C is observed for the particles ball milled for 5 h. The density and specific heat of the SiC nanofluids are determined from the mixture equations.

## 3. Technical details of tapes

The aluminium twisted tapes used in the work are of 12.5 mm width (D) and 0.8 mm thickness ( $\delta$ ). The twisted tapes (TT) with different twist ratios (TR) i.e.,  $p/D = 3, 4, 5$  are made by twisting the aluminium strips of above-mentioned dimensions; where p is the pitch as shown in the Figure 1. Some of the other aluminium strips are perforated at every 12.5 mm distance on the strip. The perforated strips are again twisted to obtain perforated twisted tapes (PTT). The twisted perforated strips are again bent to 90° to obtain an alternate axis for every

100 mm distance for different twist ratios (TR) i.e.,  $p/D = 3, 4, 5$ . The twisted tape (TT), the perforated twisted tape (PTT) and the perforated twisted tape with alternate axis (PATT) are shown in the Figure 2. The pitch ( $p$ ) and the width ( $D$ ) are depicted in the Figure 3, showing PTT and PATT.



Figure 1: TT's with TR = 3, 4 and 5. Figure 2: TT, PTT and PATT. Figure 3: PTT and PATT indicating pitch ( $p$ ) and width ( $D$ )

#### 4. Test facility

The copper tube in the test section is of 2600 mm in length with outer diameter of 31.8 mm and inner diameter of 28.6 mm. A Nichrome heating wire of 21-gauge and resistance of 46 Ohms is wound all over the length of the tube. The heater wire is wound with ceramic beads, which acts as electrical insulation. A constant heat flux condition is considered in the present work. The schematic representation of the experimental setup used for the present study is shown in the Figure 4.

The outer surface of the tube is brazed with twelve K-type thermocouples all along the circumference of the circular tube. Two RTD PT 100 type temperature sensors are used to measure the inlet and outlet temperatures of the tube. The asbestos and fiber glass insulation is provided over the copper pipe, to reduce the heat loss. A pressure transducer is placed to measure pressure drop along the pipe. The data acquisition (DAQ) system is connected to the test section to display temperatures, pressures, voltage and amperage. A program is written in the lab view software where all values are inputted from DAQ at each flow rate to obtain Nusselt number and heat transfer coefficient from the temperature readings. Similarly, the friction factor is obtained from the pressure drop readings.

A shell and tube heat exchanger are employed to cool the fluid coming out of the test section, using the cool water circulated through the chiller unit. The cooled fluid is again collected back in the reservoir tank and is recirculated. The flow rates at the pipe section and the heat exchanger are regulated by two rotameters with bypass valves. The rotameter on the pipe section side can measure flow rates in the range 300 L/h to 1200 L/h. A 0.5 HP pump is used to pump the fluid from the reservoir tank to the entrance of the test section.

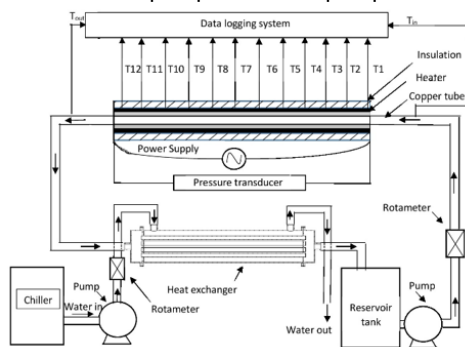


Figure 4: Schematic representation of the experimental setup

#### 5. Heat transfer and friction factor calculations

At steady state, according to the heat balance, the heat loss was found to be in between 5 % and 10 % of the electrical power input.

The heat transfer coefficient ( $h$ ) is calculated from the following equation:

$$h = mc_p (T_o - T_i) / (T_s - T_B) \quad (1)$$

$$\text{where, } T_B = \frac{(T_o + T_i)}{2}$$

An average of the twelve wall temperatures considered all along the pipe and  $T_s = (T_1 + T_2 + \dots + T_{12}) / 12$

The heat transfer rate in terms of Nusselt number ( $Nu$ ) can be written as,

$$Nu = hD/k \quad (2)$$

The friction factor is calculated from pressure drop ( $\Delta p$ ) across the tube length and is defined as,

$$f = 2\Delta p D / U^2 L \quad (3)$$

## 6. Experimental results and discussion

### 6.1 Validation tests on the base fluid in the plain tube

Under constant heat flux condition, the base fluid DIW is run in the test section at Reynolds number range of 3000 – 16000. Thereby, the temperature and pressures are recorded for calculating the Nusselt number and friction factor. Hence, to test the reliability of the test section, the obtained values are compared with the theoretical correlations available from the literature as shown in the Figure 5.

Dittus-Boelter equation (4) is employed to compare the Nusselt number as given below i.e.,

Dittus-Boelter correlation:

$$Nu = 0.023 Re^{0.8} Pr^{0.3} \quad (4)$$

Whereas, Blasius equation (5) is used to compare the friction factor as given below i.e.,

$$\text{Blasius correlation: } f = \frac{0.3164}{Re^{0.25}} \quad (5)$$

where  $3000 < Re < 5 * 10^6$  The Nusselt number and friction factor have maximum deviations of  $\pm 9.8\%$  and  $\pm 12\%$  respectively as shown in the Figure 5.

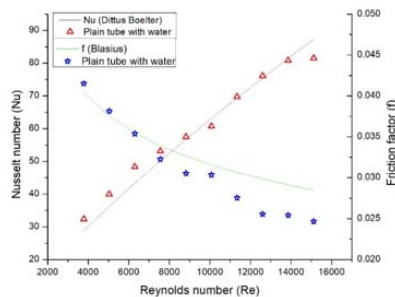


Figure 5: Validation of plain tube with the experimental data

### 6.2 Heat transfer and friction factor results

The heat transfer rate for PATT of different twist ratio (TR) = 3, 4 and 5 is shown in the Figure 6. and it can be clearly seen that the Nusselt number is increasing with a decrease in TR. The heat transfer improvement observed is around 1 % - 9.59 % in the TT with TR = 3 than that of the plain tube with nanofluid. The Nusselt number enhancement for perforated TT (PTT) and perforated TT with alternate axis (PATT) is more when compared to the regular TT as demonstrated in the Figure 8. The heat transfer increase of PTT at a TR = 3 is around 1 % - 9.3 % when compared to regular TT and is 1 % - 18 % than that of the plain tube with nanofluid. Similarly, the heat transfer augmentation of PATT at a TR = 3 is around 9.69 % - 16.13 % when compared to regular TT and is 9.7 % - 19.51 % than that of the plain tube with nanofluid. This increase in PTT and PATT can be attributed to the swirl flow due to the TT, high turbulence created due to the holes in TT for perforated TT and a change in the swirl direction periodically at each alternate axis for PATT.

Likewise, the friction factor observed is around 1.29 % - 22.5 % in the TT with TR = 3 than that of the plain tube with nanofluid. The maximum friction factor enhancement for PTT and PATT is slightly more when compared to the regular TT. The friction factor in PTT at a TR = 3 is around 1 % - 2 % more when compared to regular TT and is 1 % - 24 % more than that of the plain tube. Similarly, the friction factor in PATT at a TR = 3 is around 1 % - 8.31 % more when compared to regular TT and is 1 % - 28.9 % more than that of the plain tube with nanofluid as demonstrated in the Figure 9. The friction factor for PATT of different twist ratio (TR) = 3, 4 and 5 is shown in the Figure 7. The friction factor increase is observed in PTT and PATT as it offers flow resistance with greater pressure drop when compared to regular TT and that of the plain tube.

The fitted values of experimental data of PATT at different twist ratios in a plain tube with SiC nanofluid as in equations (6) & (7) are within  $\pm 1.5\%$  and  $\pm 2.28\%$  for Nusselt number and friction factor respectively.

$$Nu = 0.376 Re^{0.532} Pr^{0.415} TR^{-0.196} \tag{6}$$

$$f = 26.378 Re^{-0.73} TR^{-0.013} \tag{7}$$

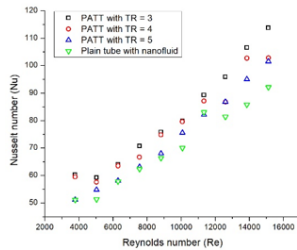


Figure 6: Effect of different TR's on Nusselt number

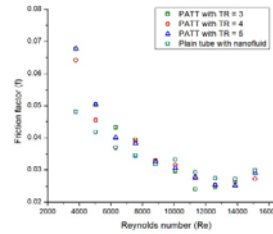


Figure 7: Effect of different TR's on friction factor vs Reynolds number in a plain tube with nanofluid

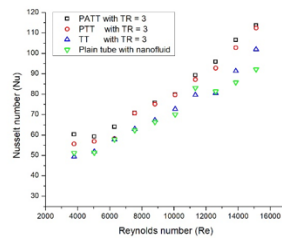


Figure 8: Effect of twist ratio on Nusselt number vs Reynolds number in a plain tube with nanofluid

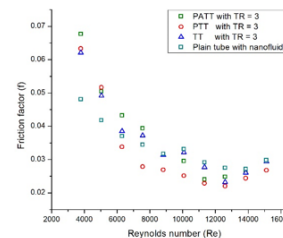


Figure 9: Effect of twist ratio on friction factor vs Reynolds number in a plain tube with nanofluid

Comparison between the Nusselt numbers and the friction factors obtained from the present experimental data with those calculated by the present regression equations of water and PATT are portrayed in Figure 10 (a) & (b).

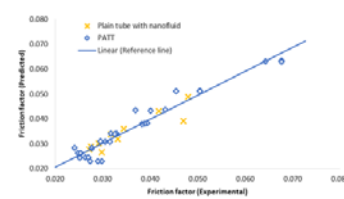
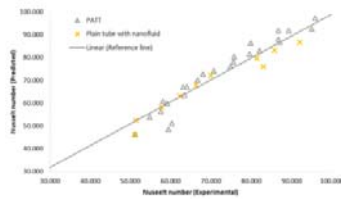


Figure 10: Comparison between experimental and predicted values (a) Nusselt numbers (b) Friction factors

### 7. Conclusions

The heat transfer rate and friction factor are analysed and compared for PATT, PTT and TT in a plain tube with nanofluid at 0.1 wt.% concentration containing SiC nanoparticles obtained after 5 h of ball milling at Reynolds number ranges between 3000 and 16000. The results obtained are summarized as below:

- The heat transfer rate and friction factor are more for PATT, PTT and TT in the decreasing order when compared with the plain tube with nanofluid.
- As the twist ratio decreases for PATT, the heat transfer rate and friction factor increase.
- The maximum heat transfer increase for PATT, PTT and TT at a TR of 3 is 19.51%, 18% and 9.59% respectively, when compared to that of the plain tube with nanofluid. Similarly, the maximum friction factor increases for PATT, PTT and TT at a TR of 3 is 28.9%, 24% and 22.5% respectively, compared to that of the plain tube. Hence, the heat transfer rate and friction factor are highest for PATT when compared to PTT and TT.

- The heat transfer enhancement is seen to be high in case of PATT, hence the regression equations are established for the Nusselt number and friction factor in case of SiC nanofluid flowing through the plain tube inserted with PATT and the attained equations are fitted with the experimental data.
- Hence, the inserts installed in the plain tube with the nanofluid flowing through it will save more energy when compared to the plain tube with water flowing through it.

### Acknowledgements

The financial support given by TEQIP-II through Ministry of Human Resource and Development (MHRD), Government of India for the research project is highly appreciated.

### References

- Amar Raj Singh Suri, Anil Kumar, Rajesh Maithani, 2018, Experimental determination of enhancement of heat transfer in a multiple square perforated twisted tape inserts heat exchanger tube, *Experimental Heat Transfer*, 31, 2, 85-105. DOI: 10.1080/08916152.2017.1397814
- Anil Kumar, Amar Raj Singh Suri, Rajesh Maithani, 2017, Effect of square wings in multiple square perforated twisted tapes on fluid flow and heat transfer of heat exchanger tube, *Case Studies in Thermal Engineering*, 10, 28–43. DOI: 10.1016/j.csite.2017.03.002
- Eiamsa-ard S., 2010, Study on thermal and fluid flow characteristics in turbulent channel flows with multiple twisted tape vortex generators, *ICHMT*, 31, 644–651. DOI: 10.1016/j.icheatmasstransfer.2010.02.004
- Eiamsa-ard S., and Wongcharee K., 2011, Friction and heat transfer characteristics of laminar swirl flow through the round tubes inserted with alternate clockwise and counter-clockwise twisted-tapes, *ICHMT*, 38, 348–352. DOI: 10.1016/j.icheatmasstransfer.2010.12.007
- Eiamsa-ard S., Saysroy A., Changcharoen W., 2018, Performance assessment of tubular heat exchanger tubes containing rectangular-cut twisted tapes with alternate axes, *Journal of Mechanical Science and Technology*, 32, 1, 433-445. DOI: 10.1007/s12206-017-1244-4
- Eiamsa-ard S., Seemawute P., 2010, Thermohydraulics of turbulent flow through a round tube by a peripherally-cut twisted tape with an alternate axis, *ICHMT*, 37, 652–659. DOI: 10.1016/j.icheatmasstransfer.2010.03.005
- Eiamsa-ard S., Thianpong C., Eiamsa-ard P., Promvong P., 2009, Convective heat transfer in a circular tube with short-length twisted tape insert, *ICHMT*, 36, 365–371. DOI: 10.1016/j.icheatmasstransfer.2009.01.006
- Eiamsa-ard S., Thianpong C., Eiamsa-ard P., Promvong P., 2010, Thermal characteristics in a heat exchanger tube fitted with dual twisted tape elements in tandem, *ICHMT*, 37, 39–46. DOI: 10.1016/j.icheatmasstransfer.2009.08.010
- Eiamsa-ard S., Wongcharee K., Eiamsa-ard P., Thianpong C., 2010, Thermohydraulic investigation of turbulent flow through a round tube equipped with twisted tapes consisting of centre wings and alternate-axes, *Experimental Thermal and Fluid Science (ETFS)*, 34, 1151–1161. DOI: 10.1016/j.expthermflusci.2010.04.004
- Li Y., Lv H., 2018, Numerical Simulation of Mass Transfer of Slug Flow in Microchannel, *Chemical Engineering Transactions*, 65, 325-330, DOI:10.3303/CET1865055
- Murugesan P., Mayilsamy K., Suresh S., Srinivasan P.S.S., 2011, Heat transfer and pressure drop characteristics in a circular tube fitted with and without V-cut twisted tape insert, *ICHMT*, 38, 329–334. DOI: 10.1016/j.icheatmasstransfer.2010.11.010
- Ponnada S., Subrahmanyam T., Naidu S.V., 2019, A comparative study on the thermal performance of water in a circular tube with twisted tapes, perforated twisted tapes and perforated twisted tapes with alternate axis. DOI: 10.1016/j.ijthermalsci.2018.11.008
- Timofeeva E.V., Smith D.S., Yu W., France D.M., Singh D., and Routbort J. L., 2010, Particle size and interfacial effects on thermo-physical and heat transfer characteristics of water-based  $\alpha$ -SiC nanofluids, *Nanotechnology*, 21, 10. DOI: 10.1088/0957-4484/21/21/215703
- Timofeeva E.V., Yu W., France D.M., Singh D., and Routbort J.L., 2011, Base fluid and temperature effects on the heat transfer characteristics of SiC in ethylene glycol/H<sub>2</sub>O and H<sub>2</sub>O nanofluids, *Journal Of Applied Physics*, 109, 1. DOI: 10.1063/1.3524274
- Wongcharee K., Eiamsa-ard S., 2011, Heat transfer enhancement by twisted tapes with alternate-axes and triangular, rectangular and trapezoidal wings, *Chem. Engineering and Processing*, 50, 211–219. DOI: 10.1016/j.cep.2010.11.012
- Yu W.H., David M. France, David S. Smith, Dileep Singh, Elena V. Timofeeva, Jules L. Routbort, 2009, Heat transfer to a silicon carbide/water nanofluid, *International Journal of Heat and Mass Transfer*, 52, 3606-3612. DOI: 10.1016/j.ijheatmasstransfer.2009.02.036